Convective heat transfer coefficients for exterior building surfaces: Existing correlations and CFD modelling

Thijs Defraeye [a, *], Bert Blocken [b] and Jan Carmeliet [c,d]

[a] *Laboratory of Building Physics, Department of Civil Engineering, Katholieke Universiteit Leuven, Kasteelpark Arenberg 40, 3001 Heverlee, Belgium*
[b] *Building Physics and Systems, Eindhoven University of Technology, P.O. Box 513, 5600 Eindhoven, The Netherlands*
[c] *Chair of Building Physics, Swiss Federal Institute of Technology Zurich (ETHZ), Wolfgang-Pauli-Strasse 15, 8093 Zürich, Switzerland*
[d] *Laboratory for Building Science and Technology, Swiss Federal Laboratories for Materials Testing and Research (Empa), Überlandstrasse 129, 8600 Dübendorf, Switzerland*

Abstract
Convective heat transfer at exterior building surfaces has an impact on the design and performance of building components such as double-skin facades, solar collectors, solar chimneys, ventilated photovoltaic arrays, etc. and also affects the thermal climate and cooling load in urban areas. In this study, an overview is given of existing correlations of the exterior convective heat transfer coefficient (CHTC) with the wind speed, indicating significant differences between these correlations. As an alternative to using existing correlations, the applicability of CFD to obtain forced CHTC correlations is evaluated, by considering a cubic building in an atmospheric boundary layer. Steady Reynolds-Averaged Navier-Stokes simulations are performed and, instead of the commonly used wall functions, low-Reynolds number modelling (LRNM) is used to model the boundary-layer region for reasons of improved accuracy. The flow field is found to become quasi independent of the Reynolds number at Reynolds numbers of about 10^5. This allows limiting the wind speed at which the CHTC is evaluated and thus the grid resolution in the near-wall region, which significantly reduces the computational expense. The distribution of the power-law CHTC-U_{10} correlation over the windward and leeward surfaces is presented (U_{10} = reference wind speed at 10 m height). It is shown that these correlations can be accurately determined by simulations with relatively low wind speed values, which avoids the use of excessively fine grids for LRNM, and by using only two or three discrete wind speed values, which limits the required number of CFD simulations.

Keywords: surface transfer coefficient, Computational Fluid Dynamics, wind speed, building, cube, correlation

---

[*] Corresponding author. Tel.: +32 (0)16321348; fax: +32 (0)16321980.
  E-mail address: thijs.defraeye@bwk.kuleuven.be

1. Introduction

The convective heat exchange at an exterior building surface, due to air flow along the surface, is usually modelled by convective heat transfer coefficients (CHTCs) which relate the convective heat flux normal to the wall $q_{c,w}$ (W/m²) to the difference between the surface temperature at the wall T_w (°C) and a reference temperature T_{ref} (°C), which is generally taken as the outside air temperature. The convective heat flux is assumed positive away from the wall. The CHTC ($h_{c,e}$ - W/m²K) is defined as:

$$h_{c,e} = \frac{q_{c,w}}{(T_w - T_{ref})} \qquad (1)$$

Convective heat transfer predictions at exterior building surfaces, by means of CHTCs, are required for several building and urban engineering applications. CHTCs are of interest for the energy performance analysis of buildings or building components, especially if they are composed of materials which have a relatively low thermal resistance (e.g. glass), resulting in a relatively high sensitivity to the CHTC. Examples are glazed buildings, double-skin facades, greenhouses, textile buildings, solar collectors, solar chimneys and ventilated photovoltaic arrays. Often, information on CHTCs is used to determine convective moisture transfer coefficients (CMTCs), by using the Chilton-Colburn analogy. Both CHTCs and CMTCs have an impact on the heat and moisture transport in the building envelope, and they are required for example to assess drying of facades, wetted by wind-driven rain [1,2] or by surface condensation by undercooling during clear cold nights [3,4]. This hygrothermal behaviour within the envelope and at the exterior surface is important for several physical, chemical and biological weathering processes such as microbiological vegetation (algae) and mould growth, reaction of deposited pollutants on the wetted surface, freeze-thaw degradation, salt transport, crystallisation and related deterioration, etc. CHTCs and CMTCs are required to predict the turbulent heat and moisture fluxes from building surfaces and streets for the analysis of the climate in urban areas with so-called mesoscale Urban Canopy Models [5-7], for example to evaluate the influence of urban heat islands on the cooling load for buildings.

CHTC correlations have been determined in the past using wind-tunnel experiments on flat plates and bluff bodies, full-scale experiments on buildings and numerical (CFD) simulations. CHTCs for buildings are often correlated to the wind speed at a reference location, for example the mean wind speed at a height of 10 m above the ground U_{10} (m/s). Linear or power-law CHTC-U correlations are mostly reported. Linear correlations account for buoyancy effects at low wind speeds, using an intercept, while power-law correlations are generally used for forced convective heat transfer.

The aim of this paper is twofold. First, an overview of the relevant research on CHTCs for exterior building surfaces is presented (section 2), from the viewpoint of building aerodynamics, i.e. the specific wind-flow pattern around a building. To the knowledge of the authors, this type of overview, including flat-plate correlations, wind-tunnel experiments on reduced-scale models, full-scale experiments and CFD simulations has not yet been performed. A recent and extensive review on CHTC correlations for applications towards solar collectors was provided by Palyvos [8]. Hagishima et al. [9] and Roy et al. [10] included a more concise overview of CHTC correlations in their work, from the viewpoint of urban canopy modelling and the greenhouse climate, respectively. In the overview in this paper, primarily additional information to existing reviews will be presented, while for other information, reference will be made to these earlier reviews.

In this overview, significant differences between the existing correlations are found, as a result from the specific conditions under which they have been derived. Thereby these correlations are only applicable under certain conditions but this is not always acknowledged by their users. As an alternative to using existing correlations, researchers or designers may also choose to determine such correlations for their specific building configuration of interest (e.g. street canyon), by means of CFD for example. Therefore, as a second part of this study (section 3), the use of CFD for the analysis of forced convective heat transfer at exterior building surfaces is evaluated by considering the case of an isolated cubic building in a neutral atmospheric boundary layer (ABL). The main focus of this part is on establishing a computationally economical approach to determine CHTC-U_{10} correlations for a specific building configuration by CFD simulations, i.e. with a minimum number of CFD simulations and without the use of excessively fine grids in the boundary-layer region. In addition, the distribution of the CHTC over the windward and leeward surfaces is presented. In section 4, the conclusions are given.

2. Existing correlations

2.1. Flat-plate experiments

Estimations of CHTCs for exterior building surfaces have often been based on CHTC-U_∞ correlations for flat plates, where U_∞ is the free-stream air speed (m/s). Some of these flat-plate correlations were based on the heat and momentum transfer analogy, using only empirical information about the flow field, and they can be represented by Eq.(2) for forced convection [11,12]:

$$\mathrm{Nu}_x = a\,\mathrm{Re}_x^{b}\,\mathrm{Pr}^{c} \tag{2}$$

where a, b and c are empirical parameters, Nu_x is the Nusselt number, based on the distance along the plate (x - m), Pr is the Prandtl number of air and Re_x is the Reynolds number, based on x and U_∞. The exponent b is about 0.8 for turbulent flow. Other flat-plate correlations were based on convective heat transfer experiments on flat plates in wind tunnels which allowed a direct determination of empirical CHTC-U_∞ correlations (e.g. [13,14]). Especially the correlations derived by Jürges [14] have been used extensively for building applications:

$$
\begin{aligned}
h_{c,e} &= 4.0 U_\infty + 5.6 & U_\infty &< 5\ \mathrm{m/s} \\
h_{c,e} &= 7.1 U_\infty^{0.78} & U_\infty &> 5\ \mathrm{m/s}
\end{aligned}
\tag{3}
$$

Jürges found a linear correlation at low speeds, also accounting for buoyancy effects, and a power-law correlation for forced convection, with an exponent approximately equal to 0.8, as in Eq.(2). Many other CHTC predictions by wind-tunnel experiments on flat plates are mentioned in a recent and extensive review by Palyvos [8], for applications towards solar collectors.

All these empirical correlations somehow lack physical similarity regarding the flow pattern, as flow along a building surface and its turbulence content can be considerably different from that along a flat plate. Thereby it is also difficult to obtain a reliable estimate of U_∞, being "some" undefined wind speed near the building surface, and usually the exact location where U_∞ is evaluated, is chosen in a rather arbitrary way. Nevertheless, a lot of valuable information about CHTCs was obtained from flat-plate experiments, for example the influence of surface roughness on the CHTC, and the obtained correlations were for a long time considered sufficient for practical purposes.

2.2. Full-scale experiments

The need for more accurate and truthful estimates of CHTCs for buildings led to an extensive amount of field measurements for building facades [15-26], for roofs [24,27,28] and to study the effect of glazing framework on the CHTC [29-31]. A clear overview of the different experimental techniques to determine these CHTCs and their limitations was given by Hagishima et al. [9]. CHTCs were also determined for greenhouses of which a concise review can be found in Roy et al. [10]. For solar collectors, the CHTC has been investigated by Shakerin [32] and Sharples and Charlesworth [33], to mention a few. An extensive review, specifically for this application, can be found in Palyvos [8].

Based on these experimental data, the CHTC could be correlated with the wind speed at a reference location. The most commonly used reference wind speeds are: (1) the wind speed in the undisturbed flow at a height of 10 m above the ground (U_{10}), which is the standard arrangement for weather station anemometers; (2) the wind speed at some distance above the roof (U_R); and (3) the wind speed near the building surface (U_S). Both linear and power-law correlations were reported. A summary of the obtained correlations, for building facades, and of the experimental conditions is given in Table 1. These correlations are presented in Figure 1-3 for the windward surface as a function of U_{10}, U_R and U_S, respectively. For some studies, only the most relevant correlations could be included due to space limitations but the remainder of them can be found in the original papers. Significant differences are found between different empirical correlations which are to some extent related to the limitations of the experiments:

- The CHTC was only measured at one or a limited number of locations on a building surface. Thereby a detailed distribution of the CHTC over the surface was not taken into account in the correlations, although measurements [17,20,24] did show that the CHTC is strongly dependent on the measuring location. Although an actual surface-averaged CHTC was not obtained, these

point-wise CHTC data are often used as if they are valid for an entire surface. Such limited spatial resolution, however, is characteristic for full-scale experiments.

- The CHTC at a certain location on the surface, and also U_S or U_R, are in reality related to the specific flow field near the building surface. The measurements of all these parameters are therefore case-specific: their values are influenced by the specific building geometry, building surroundings and location of the measurement positions. These influences are embedded in the CHTC-U correlations, which are therefore also case-specific.
- Apart from the work of Hagishima and Tanimoto [24], the influence of turbulent fluctuations on the CHTC has not been taken into account in the correlations.
- The influence of the wind direction was generally taken into account by classifying a surface as windward or leeward, where windward covers the whole range of wind directions with incidence angles from -90° to 90°. The incidence angle is defined as the angle between the approach flow wind direction and the normal to the windward surface. Lui and Harris [26] however showed that a more detailed dependency on the wind direction is required.
- Mostly smooth surfaces were considered in the analyses and the influence of different surface roughness on the CHTC was not addressed.
- Due to the difference in thermal stratification of the atmospheric boundary layer (ABL) during daytime or nighttime, the flow field around the building and thus the obtained correlation depended to some extent on the measuring period, especially for low wind speeds.

Although full-scale experiments can provide realistic CHTC data for exterior building surfaces, the large variety in building configurations, boundary conditions and experimental setups usually resulted in quite case-specific correlations which are not always applicable for other types of buildings and other boundary conditions.

2.3. Wind-tunnel experiments

A significant amount of research has been performed by wind-tunnel experiments of convective heat transfer of isolated bluff bodies, mostly cubes, placed in a turbulent boundary layer [16,34-42]. In contrast to full-scale experiments, detailed information of the distribution of the CHTC over each surface, its relation with the flow field and the dependency on flow direction was provided. Surface-averaged values of the CHTC and their correlation with the air speed were mostly reported, providing a better estimate of the overall heat loss from a surface than the single-point measurements in full-scale experiments. The obtained correlations and the experimental conditions are presented in Table 2. Note that some correlations (obtained with the naphthalene sublimation technique) rely on the analogy between heat and mass transfer to estimate the CHTC [35,36,42]. A remarkable correspondence is found for the exponent b (Eq.(2)), especially for windward (b ≈ 0.53) and leeward (b ≈ 0.66) surfaces.

Since most of these experiments were not performed in the context of building engineering/building aerodynamics, they were usually carried out for rather thin turbulent boundary layers, with respect to the body height, and at relatively low Reynolds numbers, compared to those typically encountered for buildings. These boundary conditions limit the applicability of these CHTC correlations for exterior building surfaces, although this type of (wind-tunnel) experiments itself is very valuable to determine CHTCs.

Note that, apart from wind-tunnel experiments on isolated bluff bodies, a significant amount of research has been done (not mentioned in Table 2) on the determination of CHTCs/CMTCs for urban surfaces, such as street canyons (e.g. [43-45]), for which corresponding references can be found in Hagishima et al. [9].

2.4. Numerical methods

Recently, Computational Fluid Dynamics was used to predict convective heat transfer at exterior building surfaces [46-48]. The main advantages of CFD for this application are that: (1) a specific and complex building or building configuration can be analysed; (2) very high spatial resolution data are obtained; (3) high Reynolds number flows for atmospheric conditions (10^5-10^7) can be considered and (4) detailed information on the flow field as well as the thermal field is available. In these previous studies, this allowed for a detailed analysis of: the CHTC distribution over building surfaces; the influence of turbulence and wind direction; the correlation with different reference wind speeds (U_{10}, U_S); the thermal boundary layer etc. However, some important limitations of the applied numerical models have to be emphasised.

The previous studies used the steady Reynolds-Averaged Navier-Stokes (RANS) equations to model the flow and the temperature field, combined with wall functions [46] or low-Reynolds number modelling (LRNM) [47,48] for boundary-layer modelling. Steady RANS however generally leads to less accurate flow predictions around bluff bodies, in zones of separation and recirculation [49-53], compared to unsteady RANS or Large-Eddy simulations, due to steady-flow and turbulence modelling. Steady RANS with LRNM was recently evaluated in a CFD validation study [48] using wind-tunnel measurements of convective heat transfer on the surfaces of a cube placed in turbulent channel flow at a Reynolds number of $4.6x10^3$, based on the cube height and the bulk velocity. The simulations produced accurate CHTC predictions for the windward surface (within the experimental uncertainty of 5 %), except at the edge zones which was however attributed to the limited resolution of the experiments in these zones. For the leeward surface, the predictions of the CHTC agreed to a lesser extent with experimental data (within the experimental uncertainty of 10 %, except at the edge zones). For the side and top surfaces, CHTC predictions, both distribution and surface-averaged values, were less accurate which was attributed to steady-flow and turbulence modelling of the actual transient flow features.

In contrast to LRNM, wall functions model the lower part of the boundary layer, instead of resolving it. The standard wall functions [54] are derived for equilibrium boundary layers. Therefore they are expected to produce less accurate results for complex flow problems and should be avoided when considering convective heat transfer at the wall [50,55]. Note that modified wall functions have been proposed (e.g. [56]), which can improve convective heat transfer predictions for more complex flows to some extent. LRNM, as an alternative to wall functions, requires grids with a much higher cell density in the near-wall region (e.g. 160 μm cells [47]), and it is not always feasible to generate such grids for complex building geometries in high-Reynolds-number ABL flow. Moreover, LRNM models generally do not account for surface roughness.

The CHTC-U_{10} correlations from previous CFD studies are presented in Table 3. All correlations agree quite well (within 10 %) in the U_{10} range of 1-15 m/s, mainly due to the similarity in building configuration and boundary conditions. Although standard wall functions were found to provide significant overestimations of the CHTC [47,48], the correlation of Emmel et al. [46] shows a good agreement with the LRNM results. This is attributed to the fact that the overestimation of the CTHC by the wall functions is almost completely balanced by the underestimation of the CHTC due to an unrealistically low inlet turbulence level imposed by Emmel et al. [46], as explained and demonstrated by Blocken et al. [47]. Note also that the imposed inlet turbulence level of Blocken et al. [47] and Defraeye et al. [48] differed slightly.

Due to the ease of use and availability of CFD compared to other techniques (e.g. wind tunnel) and due to the significant differences found for the existing correlations (sections 2.1 - 2.4), researchers or engineers could prefer obtaining their own CHTC correlations for a specific building configuration of interest (e.g. street canyon) with CFD, instead of using existing correlations. As mentioned, steady RANS with LRNM can be successfully used to determine such exterior CHTCs for certain specific cases, e.g. windward and leeward surfaces of an isolated building [48]. There are however some limitations to the practical use of this methodology for obtaining CHTC-U_{10} correlations for a specific building configuration: (1) steady RANS implies less accurate flow modelling in regions of recirculation and separation (e.g. top and side surfaces of a cube); (2) no surface roughness is accounted for with LRNM; (3) for LRNM, a very high grid resolution is required in the near-wall region at high Reynolds numbers; and (4) several simulations are required at different wind speeds to obtain the correlations. The first two limitations are inherent to steady RANS with LRNM but regarding the last two limitations, improvements can be made: this paper focuses on establishing a computationally economical approach to determine CHTC-U_{10} correlations by CFD simulation (steady RANS with LRNM), i.e. without the use of excessively fine grids in the boundary-layer region and with a minimum number of CFD simulations. The building configuration that is considered for this analysis is an isolated cubic building in a neutral ABL where the forced CHTCs on the exterior surfaces are evaluated for an incidence angle of 0° (wind direction perpendicular to one of the surfaces).

3. CFD modelling of CHTCs for a cubic building in an ABL

3.1. Numerical model

A cubic building with a height (H) of 10 m is considered. The size of the computational domain is determined according to the guidelines of Franke et al. [57] and Tominaga et al. [58] and is presented in Figure 4. The blockage ratio is 1.5 %. At the inlet of the domain, the vertical profiles of the mean

horizontal wind speed U (logarithmic law), turbulent kinetic energy (k - m²/s²) and turbulent dissipation rate (ε - m²/s³) are imposed, according to Richards and Hoxey [59], representing a neutral ABL, i.e. where turbulence in the ABL originates only from friction and shear and not from thermal stratification:

$$U(z) = \frac{u^*_{ABL}}{\kappa} \ln(\frac{z+z_0}{z_0})$$

$$k = 3.3 u^{*2}_{ABL} \tag{4}$$

$$\varepsilon = \frac{u^{*3}_{ABL}}{\kappa(z+z_0)}$$

where u^*_{ABL} is the ABL friction velocity (m/s), κ is the von Karman constant (0.4187), z is the height above the ground (m) and z_0 is the aerodynamic roughness length (m). The friction velocity is linked to a reference wind speed, namely U_{10} in this study, which is taken equal to 0.5 m/s. Note that other wind speeds (U_{10} = 0.005 - 7.5 m/s) are also evaluated in sections 3.3 and 3.4.2. The parameter z_0 is 0.03 m, which corresponds to a land surface with low vegetation (e.g. grass) and isolated obstacles [60]. Wind is blowing perpendicular to the windward surface. The temperature of the approach flow is 10°C, which is taken as the reference temperature in Eq.(1). From the ABL temperature profiles over a flat terrain [61], it can be shown that assuming a constant temperature over the height of the ABL is a relatively good approximation for a neutral ABL with a zero heat flux at the ground and if a limited height is considered (60 m in this case).

The ground boundary is modelled as a no-slip boundary with zero roughness since surface roughness values can not be specified if LRNM is used [62], which is one of the major drawbacks of using the LRNM approach. This restriction will inevitably introduce streamwise gradients in the vertical profiles of mean horizontal wind speed and turbulence [63] but this could not be avoided. This change in the vertical profiles was assessed by performing a CFD simulation in an empty computational domain. This simulation is not reported in this paper but showed a distinct change in the profiles in the first meters near the ground surface, which alters the flow field around the cube to some extent. The ground boundary is taken adiabatic. The exterior surfaces of the building are modelled as no-slip boundaries with zero roughness and have an imposed constant temperature of 20°C.

For the top boundary of the computational domain, a symmetry boundary condition (slip wall) is used, which assumes that the normal velocity component and the normal gradients at the boundary are zero. Note that other ways to model the top boundary in a more optimised way have been reported by Blocken et al. [63]. This modelling technique however is considered less important in the present case, since a relatively short upstream fetch is considered. Zero static pressure is imposed at the outlet. For the lateral boundaries, periodic boundary conditions are used.

An appropriate grid is built, based on a grid sensitivity analysis. For the estimation of the discretisation error, the grid convergence index is used, as proposed by Roache [64] and extended by Eça and Hoekstra [65]. The average discretisation error over the windward surface is about 5 % for the CHTC. The grid is a hybrid grid (hexahedral and prismatic cells) consisting of about 2.0×10^6 cells (Fig. 4).

In order to resolve the boundary layer appropriately, LRNM grids require a high cell density in the wall-normal direction and a small y^+ value (dimensionless wall distance) of the wall-adjacent cell ($y^+ \approx 1$), compared to wall functions ($30 < y^+ < 500$), where y^+ is defined as:

$$y^+ = \frac{\sqrt{\frac{\tau_w}{\rho}} y_P}{\nu} \tag{5}$$

where y_P is the distance (normal) of centre point P of the wall-adjacent cell to the wall (m), τ_w is the shear stress at the wall (kg/ms²), ρ is the air density (kg/m³) and ν is the kinematic viscosity of air (m²/s). The highest y^+ values are attained at the edges of the windward surface but are smaller than 3.

Since τ_w increases with increasing velocity (U_{10}), the evaluation of higher wind speeds with LRNM (sections 3.3 and 3.4.2) requires that the grid is locally refined in the boundary-layer region, hence lowering y_P, in order to retain a y^+ of about 1. Thereby, the required y_P can become very small at high Reynolds numbers (+/- 0.05 mm for U_{10} = 7.5 m/s) which can entail considerable problems for grid generation and convergence rate. Therefore, it is investigated in this paper if, for LRNM purposes, low

wind speeds, and hence a relatively large y_P, can be used to determine CHTC-U_{10} correlations (see sections 3.3 and 3.4.2).

3.2. Numerical simulation

The simulations are performed with the CFD package Fluent 6.3, which uses the control volume method. Steady RANS is used in combination with a turbulence model. The realizable k-ε model [66] is used together with LRNM to take care of the viscosity-affected region, for which the one-equation Wolfshtein model [67] is used. Note that this realizable k-ε turbulence model with LRNM was evaluated in the previously mentioned CFD validation study (section 2.4, [48]) where a good agreement with experimental data was obtained for both windward and leeward surfaces. Based on the results of this validation study, the focus will be only on these two surfaces.

The focus of this paper is on forced convection where the possibility of using low speeds to determine CHTC-U_{10} correlations, for LRNM purposes, is investigated. Therefore, buoyancy effects are not taken into account in the simulations, since they will otherwise affect the air flow field at such low Reynolds numbers. Radiation is also not considered in the simulations since the focus was only on forced convection, and fixed temperature boundary conditions are used for the building surfaces.

Second-order discretisation schemes are used throughout. The SIMPLE algorithm is used for pressure-velocity coupling. Pressure interpolation is second order. Convergence was assessed by monitoring the velocity, turbulent kinetic energy and temperature on specific locations in the flow field and heat fluxes on the surface of the cube.

3.3. Reynolds number dependence of the flow field

The intention is to determine the forced CHTC-U_{10} correlations at relatively low U_{10} (Reynolds numbers), without compromising their accuracy for use at higher U_{10}. The motivation for using low U_{10} is computational economy when using the fine LRNM grids. To allow extrapolation to higher U_{10}, Reynolds number independence should be achieved. This implies that the overall flow field around the building at low U_{10} is similar to that found at higher Reynolds numbers ($U_{10} = 5 - 15$ m/s), typical for forced convective ABL flow. Otherwise, the CHTC distribution over the different surfaces will differ. For sharp-edged bluff bodies, which have fixed separation points, namely the edges, and which are immersed in deep turbulent boundary layers, such as the ABL, it is generally assumed in wind-tunnel testing that the flow field becomes independent of the Reynolds number once a certain Reynolds number is exceeded. This threshold value is called the critical Reynolds number, Re_{cr}. Reynolds number independence was confirmed by wind-tunnel experiments [68-75] and the corresponding Re_{cr} values, based on the building height (H) and the wind speed at that height (U_H), are reported in Table 4. Note however that most of these experiments were not always extensive studies on this Reynolds number effect or were performed for a restricted Reynolds number range. Some studies [75-77] showed that Reynolds number dependency is influenced by wind direction, building geometry and the location on the surface and that it can differ for mean and fluctuating flow quantities, which could partially explain the differences found in Table 4.

Since this study specifically aims at determining the CHTC at low wind speeds, for LRNM purposes, the Reynolds number dependency in the numerical simulations is investigated by analysing the flow field at different wind speeds, namely for $U_{10} = 0.005, 0.05, 0.15, 0.5$ and 5 m/s, resulting in Reynolds numbers of 3.5×10^3 to 3.5×10^6, based on the building height H and U_{10}. Note that the focus is on the overall flow field, not on the flow in the boundary layer near the building surface. Since the simulations are steady, any Reynolds number dependency by unsteady behaviour (e.g. vortex shedding) is not captured.

The dimensionless mean horizontal wind speed and turbulent kinetic energy along the centreline through the building are reported in Figure 5. Apart from the flow field, pressure coefficients are frequently used to evaluate the Reynolds number dependency. Therefore, the mean pressure coefficients C_P ($= (p-p_0)/(0.5\rho U_{10}^2)$) with p = mean pressure at the surface and p_0 = atmospheric pressure) in a vertical centreplane on the windward and leeward surfaces are reported in Figure 6. A significant dependency on the flow field can be noticed at low Reynolds numbers (i.e. $U_{10} = 0.005$ m/s and 0.05 m/s). The small differences between the results for $U_{10} = 5$ m/s and the results for $U_{10} = 0.15$ m/s and 0.5 m/s are attributed to the slightly different grid (in the boundary-layer region) that is used in the simulations for high wind speeds (5 m/s). It can be concluded that, for this type of numerical simulations (steady RANS with LRNM), the overall flow field is quasi independent of the Reynolds number, from Reynolds numbers exceeding about 10^5 ($U_{10} = 0.15$ m/s), which is comparable to the highest Re_{cr} values found in Table 4. This lower limit will be taken into account when establishing the correlations in section 3.4.2. Note that

7

aerodynamic bodies (e.g. cylindrical buildings) will show a Reynolds number dependency up to higher Reynolds numbers because for such bodies the positions of the separation points are Reynolds-number dependent.

3.4. CHTC predictions and correlations

3.4.1. Distribution of CHTC over surfaces

A major advantage of using CFD to predict CHTCs is that high spatial resolution data are obtained. The distribution of $(h_{c,e}-h_{c,e,avg})/h_{c,e,avg}$ over the windward and leeward surfaces is reported in Figure 7 for $U_{10} = 0.5$ m/s, where $h_{c,e,avg}$ represents the surface-averaged CHTC. Differences with the surface-averaged CHTC of about 25 % are found. For both surfaces, the surface-averaged value is found at 0.7H in the vertical centreplane, which is very close to the stagnation point for the windward surface. The wind-tunnel experiment of Meinders et al. [39] on a wall-mounted cube showed comparable locations for the surface-averaged CHTC for both windward and leeward surfaces, respectively at 0.62H and 0.55H. Note that the exact location is dependent on the approach flow conditions.

3.4.2. CHTC-U_{10} correlation

Simulations at different wind speeds are performed to obtain correlations of the forced CHTC with the mean wind speed, U_{10}, for the windward and leeward surfaces. Correlations with U_S or U_R are not reported since these wind speeds are strongly related to the specific flow field around the building, which makes the obtained correlations less useable for other building geometries. U_{10} on the other hand is taken outside the wind-flow pattern that is disturbed by the presence of the building. Values of U_{10} are generally available from measurements at a meteorological station. The evaluated wind speeds, U_{10}, are 0.05, 0.15, 0.5, 1, 2.5, 5 and 7.5 m/s. Based on the findings of section 3.3, only correlations with wind speeds higher than 0.15 m/s are quasi free of Reynolds number effects.

Since the simulations focus on forced convection, a power-law correlation between the CHTC and U_{10} is more appropriate and also provides a better approximation of the data, compared to a linear one:

$$h_{c,e} = AU_{10}^B \tag{6}$$

where A and B are respectively a coefficient and exponent, where the exponent determines the shape of the curve. The values of this coefficient and exponent (for U_{10} from 0.15 m/s to 7.5 m/s) are represented in Figure 8 and 9 over the windward and leeward surfaces. Note that the z-axis in Figure 8(b)-9(b) is reversed compared to that in Figure 8(a)-9(a). For the windward surface, the exponent B does not vary a lot except for the zone near the ground surface. The coefficient A increases from the bottom to the top of the windward surface. For the leeward surface, the exponent B increases from bottom to top and the coefficient A shows a maximum at z/H = 0.3 (at x/H = 0.5) after which it decreases towards the bottom and top of the surface.

Often, a single, and preferably surface-averaged, value of the CHTC is requested in practical applications. The correlation of the surface-averaged CHTC with U_{10} (from 0.15 m/s to 7.5 m/s) for both surfaces is given by:

$$h_{c,e,avg} = 5.01U_{10}^{0.85}(WW)$$
$$h_{c,e,avg} = 2.27U_{10}^{0.83}(LW) \tag{7}$$

Note that the exponent B is comparable to what was found for flat plates (0.8). A comparison with other correlations (Table 1 and Table 2) is not always justified since CHTC-U_{10} correlations are dependent on factors such as the building surroundings, building geometry, position on the surface, surface roughness and wind direction. The correlations derived in this paper are only valid for the windward and leeward surfaces of an isolated cubic body in a neutral ABL for an incidence angle of 0° at high Reynolds and low Richardson numbers, or comparable configurations.

To obtain such correlations for other building configurations with CFD, it would be convenient if the CHTCs only have to be evaluated at a few wind speeds, to reduce the number of simulations, and for relatively low wind speeds to have an acceptable y_P for LRNM purposes, but free of Reynolds number effects. Therefore the influence of the number of simulations, used to determine the CHTC-U_{10} correlations, and of the required magnitude of the wind speed (U_{10}) in the simulations, on the accuracy of

the obtained correlations is investigated. For this, surface-averaged CHTC data from CFD ($h_{c,e,avg}$) for the windward surface are used to compose several CHTC-U_{10} correlations (cases) by approximation, by only using CHTC data at a limited number of wind speeds U_{10} (predominantly low wind speeds and a low number of wind speeds). The accuracy of such a specific CHTC-U_{10} correlation is evaluated by comparing the surface-averaged CHTC, predicted by the correlation ($h_{c,e,avg,corr}$), to the actual CHTC data ($h_{c,e,avg}$) at several wind speeds. The difference $\left| h_{c,e,avg,corr} - h_{c,e,avg} \right| / h_{c,e,avg}$ is presented in Table 5 for these different cases. Note that accurate CHTC-U_{10} correlations by using CFD data at low wind speeds should also provide accurate predictions for higher wind speeds (Reynolds numbers).

Case A, in Table 5, is composed using all evaluated wind speeds which are quasi free of Reynolds number effects and therefore obviously gives a good approximation over the whole range of wind speeds. At $U_{10} = 0.05$ m/s, a large difference is found, which is attributed to Reynolds number effects. If this wind speed is used in a correlation (case B), large errors are therefore found when extrapolating to high U_{10}. For case C and D, still observable extrapolation errors are found at high wind speeds. Since case E (0.5 - 1 m/s) provides a much more accurate extrapolation, the errors for case C and case D could be attributed to a remaining, but small, Reynolds dependency for $U_{10} = 0.15$ m/s. It is shown that correlations with two wind speeds (case E and case F) and with relatively low wind speeds can provide accurate estimates of the CHTC and do not necessarily have to cover a large Reynolds number range. Note that these wind speeds are about a factor 10 lower that those found for a typical forced convective ABL. This implies that the grid resolution in the boundary layer can roughly be taken a factor 10 coarser. Based on this study, it is advised that, if CHTC-U_{10} correlations for sharp-edged buildings in turbulent boundary layers are obtained with CFD, simulations are made with at least two wind speeds corresponding to a minimum Reynolds number of about $3x10^5$ and where the lowest and highest wind speed differ with at least a factor 2.

4. Conclusions

In a first part, an overview of the research on CHTC correlations for exterior building surfaces was given and some limitations of each methodology were identified. A large variation in the CHTC-U correlations was found, which was related to the specific conditions under which each correlation was derived, limiting to some extent their applicability for other building configurations.

In a second part, an alternative to using existing CHTC-U correlations was explored, namely the use of CFD for the prediction of forced CHTCs for a specific building configuration. The focus was on an isolated cubic building in a neutral ABL at an incidence angle of 0°. Only the windward and leeward surfaces were considered since an earlier validation study showed that accurate CHTC predictions could be obtained here with steady RANS if combined with LRNM, instead of the commonly used wall functions.

The aim of this study was to improve the practical use of steady RANS with LRNM to obtain CHTC-U_{10} correlations. For steady RANS and for a sharp-edged building, the overall flow field was found to become quasi independent of the Reynolds number at Reynolds numbers of about 10^5, based on H and U_{10}. Thereby the CHTC-U_{10} correlations could be determined by using relatively low wind speeds ($U_{10} \approx$ 1 m/s), which avoids the use of excessively fine grids for LRNM, and still provide a good approximation for higher wind speeds by extrapolation. Moreover, evaluating only two or three wind speeds was found to be sufficient to provide accurate correlations, which reduces the required number of CFD simulations.

Furthermore the CHTC was found to vary significantly across windward and leeward surfaces and the CHTC was found to be equal to the surface-averaged CHTC at a height of approximately 0.7H for both surfaces. The local CHTC-U_{10} (power-law) correlation (Eq.(6)) was characterised by an exponent B which was quasi-constant for the windward surface, but which varied significantly over the leeward surface.

Conflict of interest statement
The authors of the manuscript entitled: "Convective heat transfer coefficients for exterior building surfaces: Existing correlations and CFD modelling" do not have any conflict of interest.

stimulates industrial research and technology transfer in the Flemish industry. Their contribution is gratefully acknowledged.

References

[1] B. Blocken, S. Roels, J. Carmeliet, A combined CFD-HAM approach for wind-driven rain on building facades, J. Wind Eng. Ind. Aerodyn. 95 (7) (2007) 585-607.

[2] H. Janssen, B. Blocken, S. Roels, J. Carmeliet, Wind-driven rain as a boundary condition for HAM simulations: analysis of simplified modelling approaches, Build. Environ. 42 (4) (2007) 1555-1567.

[3] D. Camuffo, R. Giorio, Quantitative evaluation of water deposited by dew on monuments, Bound.-Lay. Meteorol. 107 (3) (2003) 655-672.

[4] D. Aelenei, F.M.A. Henriques, Analysis of the condensation risk on exterior surface of building envelopes, Energ. Buildings 40 (10) (2008) 1866-1871.

[5] V. Masson, A physically-based scheme for the urban energy budget in atmospheric models, Bound.-Lay. Meteorol. 94 (3) (2000) 357-397.

[6] H. Kusaka, H. Kondo, Y. Kikegawa, F. Kimura, A simple single-layer urban canopy model for atmospheric models: comparison with multi-layer and slab models, Bound.-Lay. Meteorol. 101 (3) (2001) 329-358.

[7] H. Kondo, Y. Genchi, Y. Kikegawa, Y. Ohashi, H. Yoshikado, H. Komiyama, Development of a multi-layer urban canopy model for the analysis of energy consumption in a big city: structure of the urban canopy model and its basic performance, Bound.-Lay. Meteorol. 116 (3) (2005) 395-421.

[8] J.A. Palyvos, A survey of wind convection coefficient correlations for building envelope energy systems' modelling, Appl. Therm. Eng. 28 (8-9) (2008) 801-808.

[9] A. Hagishima, J. Tanimoto, K. Narita, Intercomparisons of experimental convective heat transfer coefficients and mass transfer coefficients of urban surfaces, Bound.-Lay. Meteorol. 117 (3) (2005) 551-576.

[10] J.C. Roy, T. Boulard, C. Kittas, S. Wang, PA - Precision Agriculture: convective and ventilation transfers in greenhouses, Part 1: the greenhouse considered as a perfectly stirred tank, Biosyst. Eng. 83 (1) (2002) 1-20.

[11] T. Cebeci, P. Bradshaw, Physical and Computational aspects of Convective Heat Transfer, first ed., Springer-Verlag, New York, 1984.

[12] J.H. Lienhard IV, J.H. Lienhard V, A Heat Transfer Textbook, third ed., Phlogiston Press, Cambridge Massachusetts, 2006.

[13] W. Nusselt, W. Jürges, The cooling of a flat wall by an airstream (Die Kühlung einer ebenen wand durch einen Luftstrom), Gesundh.-Ing. 52 (45) (1922) 641-642.

[14] W. Jürges, The heat transfer at a flat wall (Der Wärmeübergang an einer ebenen Wand), Beihefte zum Gesundh.-Ing. 1 (19) (1924).

[15] K. Gerhart, Model experiments on the distribution of convective heat transfer at building facades (Modellversuche über die verteilung des konvektiven wärmeüberganges an gebäudefassaden), Kältetechn.-Klimatisier. 19 (5) (1967) 122-128. (as cited by [20])

[16] N.S. Sturrock, Localised boundary layer heat transfer from external building surfaces, PhD Thesis, University of Liverpool, 1971. (as cited by [20])

[17] N. Ito, K. Kimura, J. Oka, A field experiment study on the convective heat transfer coefficient on exterior surface of a building, ASHRAE Trans. 78 (1) (1972) 184-191.

[18] ASHRAE, ASHRAE Task Group, Procedure for determining heating and cooling loads for computerising energy calculations, Algorithms for building heat transfer subroutines, New York, 1975. (as cited by [20])

[19] K. Nicol, The energy balance of an exterior window surface, Inuvik, N.W.T., Canada, Build. Environ. 12 (4) (1977) 215-219.

[20] S. Sharples, Full-scale measurements of convective energy losses from exterior building surfaces, Build. Environ. 19 (1) (1984) 31-39.

[21] M. Yazdanian, J. H. Klems, Measurement of the exterior convective film coefficient for windows in low-rise buildings, ASHRAE Trans. 100 (1) (1994) 1087-1096.

[22] S.E.G. Jayamaha, N.E. Wijeysundera, S.K. Chou, Measurement of the heat transfer coefficient for walls, Build. Environ. 31 (5) (1996) 399-407.

[23] D.L. Loveday, A.H. Taki, Convective heat transfer coefficients at a plane surface on a full-scale building facade, Int. J. Heat Mass Tran. 39 (8) (1996) 1729-1742.

[24] A. Hagishima, J. Tanimoto, Field measurements for estimating the convective heat transfer coefficient at building surfaces, Build. Environ. 38 (7) (2003) 873-881.

[25] L. Zhang, N. Zhang, F. Zhao, Y. Chen, A genetic-algorithm-based experimental technique for determining heat transfer coefficient of exterior wall surface, Appl. Therm. Eng. 24 (2-3) (2004) 339-349.

[26] Y. Liu, D.J. Harris, Full-scale measurements of convective coefficient on external surface of a low-rise building in sheltered conditions, Build. Environ. 42 (7) (2007) 2718-2736.

[27] R.D. Clear, L. Gartland, F.C. Winkelman, An empirical correlation for the outside convective air-film coefficient for horizontal roofs, Energ. Buildings 35 (8) (2003) 797-811.

[28] J. Shao, J. Liu, J. Zhao, W. Zhang, D. Sun, Z. Fu, A novel method for full-scale measurement of the external convective heat transfer coefficient for building horizontal roof, Energ. Buildings 41 (8) (2009) 840-847.

[29] D.L. Loveday, A.H. Taki, H. Versteeg, Convection coefficients at disrupted building facades: laboratory and simulation studies, Int. J. Ambient Energ. 15 (1) (1994) 17-26.

[30] A.H. Taki, D.L. Loveday, External convection coefficients for framed rectangular elements on building facades, Energ. Buildings 24 (2) (1996) 147-154.

[31] A.H. Taki, D.L. Loveday, Surface convection coefficients for buildings facades with vertical mullion-type protrusions, Proc. Inst. Mech. Eng. - Part A: J. Power Energy 210 (2) (1996) 165-176.

[32] S. Shakerin, Wind-related heat transfer coefficient for flat-plate solar collectors, Trans. ASME: J. Sol. Energ. 109 (1987) 108-110.

[33] S. Sharples, P.S. Charlesworth, Full-scale measurements of wind-induced convective heat transfer from a roof-mounted flat plate solar collector, Sol. Energy 62 (2) (1998) 69-77.

[34] W.J. Kelnhofer, C.J. Thomas, External convection heat transfer coefficients on a building model, ASME Paper 76-WA/FE-30, in: Proceedings of the ASME Winter Annual Meeting, New York, USA, 1976.

[35] M.K. Chyu, V. Natarajan, Local heat/mass transfer distributions on the surface of a wall-mounted cube, Trans. ASME: J. Heat Trans. 113 (4) (1991) 851-857.

[36] V. Natarajan, M.K. Chyu, Effect of flow angle-of-attack on the local heat/mass transfer from a wall-mounted cube, Trans. ASME: J. Heat Trans. 116 (3) (1994) 552-560.

[37] D.A. Quintela, D.X. Viegas, Convective heat losses from buildings, in: J.E. Cermak, A.G. Davenport, E.J. Plate, D.X. Viegas (Eds.), Wind Climate in Cities, Kluwer Academic Publishers, The Netherlands, 1995, pp. 503-522.

[38] E.R. Meinders, Experimental study of heat transfer in turbulent flows over wall-mounted cubes, PhD thesis, Technische Universiteit Delft, 1998.

[39] E.R. Meinders, K. Hanjalic, R.J. Martinuzzi, Experimental study of the local convection heat transfer from a wall-mounted cube in turbulent channel flow, Trans. ASME: J. Heat Trans. 121 (3) (1999) 564-573.

[40] H. Nakamura, T. Igarashi, T. Tsutsui, Local heat transfer around a wall-mounted cube in the turbulent boundary layer, Int. J. Heat Mass Tran. 44 (18) (2001) 3385-3395.

[41] H. Nakamura, T. Igarashi, T. Tsutsui, Local heat transfer around a wall-mounted cube at 45° to flow in a turbulent boundary layer, Int. J. Heat Mass Tran. 24 (6) (2003) 807-815.

[42] K. Wang, R. Chiou, Local mass/heat transfer from a wall-mounted block in rectangular channel flow, Heat Mass Transfer 42 (7) (2006) 660-670.

[43] J.F. Barlow, S.E. Belcher, A wind tunnel model for quantifying fluxes in the urban boundary layer, Bound.-Lay. Meteorol. 104 (1) (2002) 131-150.

[44] J.F. Barlow, I.N. Harman, S.E. Belcher, Scalar fluxes from urban street canyons part 1: laboratory simulation, Bound.-Lay. Meteorol. 113 (3) (2004) 369-385.

[45] K. Narita, Experimental study of the transfer velocity for urban surfaces with a water evaporation method, Bound.-Lay. Meteorol. 122 (2) (2007) 293-320.

[46] M.G. Emmel, M.O. Abadie, N. Mendes, New external convective heat transfer coefficient correlations for isolated low-rise buildings, Energ. Buildings 39 (3) (2007) 335-342.

[47] B. Blocken, T. Defraeye, D. Derome, J. Carmeliet, High-resolution CFD simulations for forced convective heat transfer coefficients at the facade of a low-rise building, Build. Environ. 44 (12) (2009) 2396-2412.

[48] T. Defraeye, B. Blocken, J. Carmeliet, CFD analysis of convective heat transfer at the surfaces of a cube immersed in a turbulent boundary layer, Int. J. Heat Mass Tran. 53 (1-3) (2010) 297-308.

[49] M. Murakami, A. Mochida, Y. Hayashi, Examining the k-ε model by means of a wind tunnel test and Large-Eddy simulation of the turbulence structure around a cube, J. Wind Eng. Ind. Aerodyn. 35 (1990) 87-100.

[50] S. Murakami, Comparison of various turbulence models applied to a bluff body, J. Wind Eng. Ind. Aerodyn. 46-47 (1993) 21-36.

[51] S. Murakami, A. Mochida, R. Ooka, S. Kato, S. Iizuka, Numerical prediction of flow around a building with various turbulence models: comparison of k-ε EVM, ASM, DSM and LES with wind tunnel tests, ASHRAE Trans. 102 (1) (1996) 741-753.

[52] G. Iaccarino, A. Ooi, P.A. Durbin, M. Behnia, Reynolds averaged simulation of unsteady separated flow, Int. J. Heat Fluid Fl. 24 (2) (2003) 147-156.

[53] Y. Tominaga, A. Mochida, S. Murakami, S. Sawaki, Comparison of various revised k-ε models and LES applied to flow around a high-rise building model with 1:1:2 shape placed within the surface boundary layer, J. Wind Eng. Ind. Aerodyn. 96 (4) (2008) 389-411.

[54] B.E. Launder, D.B. Spalding, The numerical computation of turbulent flows, Comput. Method. Appl. M. 3 (2) (1974) 269-289.

[55] B.E. Launder, On the computation of convective heat transfer in complex turbulent flows, Trans. ASME: J. Heat Trans. 110 (1988) 1112-1128

[56] M. Popovac, K. Hanjalic, Compound wall treatment for RANS computation of complex turbulent flows and heat transfer, Flow Turbul. Combust. 78 (2) (2007) 177-202.

[57] J. Franke, A. Hellsten, H. Schlünzen, B. Carissimo, Best practice guideline for the CFD simulation of flows in the urban environment, COST Action 732: Quality assurance and improvement of microscale meteorological models, Hamburg, 2007.

[58] Y. Tominaga, A. Mochida, R. Yoshie, H. Kataoka, T. Nozu, M. Yoshikawa, T. Shirasawa, AIJ guidelines for practical applications of CFD to pedestrian wind environment around buildings, J. Wind Eng. Ind. Aerodyn. 96 (10-11) (2008) 1749-1761.

[59] P.J. Richards, R.P. Hoxey, Appropriate boundary conditions for computational wind engineering models using the k-ε turbulence model, J. Wind Eng. Ind. Aerodyn. 46-47 (1993) 145-153.

[60] J. Wieringa, Updating the Davenport roughness classification, J. Wind Eng. Ind. Aerodyn. 41-44 (1992) 357-368.

[61] H. Panofsky, J. Dutton, Atmospheric Turbulence, Wiley, New York, 1984.

[62] Fluent Inc., Fluent 6.3 User's Guide, Lebanon - New Hampshire, 2006.

[63] B. Blocken, T. Stathopoulos, J. Carmeliet, CFD simulation of the atmospheric boundary layer: wall function problems, Atmos. Environ. 41 (2) (2007) 238-252.

[64] P.J. Roache, Perspective: a method for uniform reporting of grid refinement studies, Trans. ASME: J. Fluid. Eng. 116 (3) (1994) 405-413.

[65] L. Eça, M. Hoekstra, A verification exercise for two 2-D steady incompressible turbulent flows, in: P. Neittaanmäki, T. Rossi, M. Majava, O. Pironneau (Eds.), Proceedings of the ECCOMAS 2004, Jyväskylä, Finland, 2004.

[66] T.H. Shih, W.W. Liou, A. Shabbir, Z. Yang, J. Zhu, A new k-ε eddy viscosity model for high Reynolds number turbulent flows, Comput. Fluids 24 (3) (1995) 227-238.

[67] M. Wolfshtein, The velocity and temperature distribution in one-dimensional flow with turbulence augmentation and pressure gradient, Int. J. Heat Mass Tran. 12 (3) (1969) 301-318.

[68] W.G. Hoydysh, R.A. Griffiths, Y. Ogawa, A scale model study of the dispersion of pollution in street canyons, APCA paper 74-157, in: Proceedings of the 67th Annual Meeting of the Air Pollution Control Association, Denver, USA, 1974.

[69] I.P. Castro, A.G. Robins, The flow around a surface-mounted cube in uniform and turbulent streams, J. Fluid Mech. 79 (2) (1977) 307-335.

[70] N. J. Cherry, R. Hillier, M. E. M. P. Latour, Unsteady measurements in a separated and reattaching flow, J. Fluid Mech. 144 (1984) 13-46.

[71] M. Ohba, Experimental studies for effects of separated flow on gaseous diffusion around two model buildings, Trans. AIJ: J. Arch. Plan. Environ. Eng. 406 (1989) 21-30.

[72] N. Djilali, I.S. Gartshore, Turbulent flow around a bluff rectangular plate, Part 1: experimental investigation, Trans. ASME: J. Fluid. Eng. 113 (1991) 51-59.

[73] W.H. Snyder, Some observations of the influence of stratification on diffusion in building wakes, in: I.P. Castro, N.J. Rockliff (Eds.), Stably Stratified Flows: Flow and Dispersion over

Topography. Fourth Conference on Stably Stratified Flows: Institute of Mathematics and its Application, Clarendon Press, Oxford, U.K., 1994, pp. 301-324.

[74] A. Mochida, S. Murakami, S. Kato, The similarity requirements for wind tunnel model studies of gas diffusion, J. Wind Eng. Japan 59 (1994) 23-28.

[75] K. Uehera, S. Wakamatsu, R. Ooka, Studies on the critical Reynolds number indices for wind-tunnel experiments on flow within urban areas, Bound.-Lay. Meteorol. 107 (2) (2003) 353-370.

[76] H.C. Lim, I.P. Castro, R.P. Hoxey, Bluff bodies in deep turbulent boundary layers: Reynolds number issues, J. Fluid Mech. 571 (2007) 97-118.

[77] S. Song, J.K. Eaton, Reynolds number effects on a turbulent boundary layer with separation, reattachment, and recovery, Exp. Fluids 36 (2) (2004) 246-258.
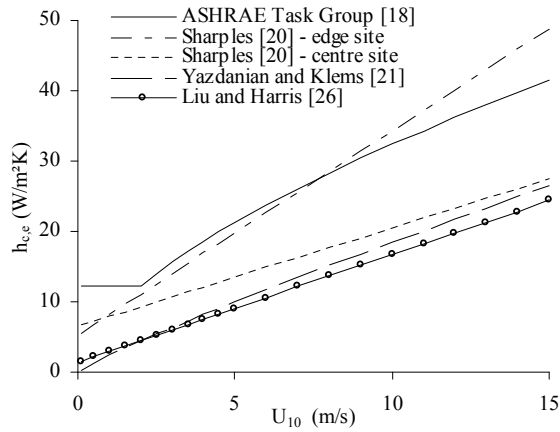
Figures

Fig. 1. CHTC-U_{10} correlations for building facades from previous research.
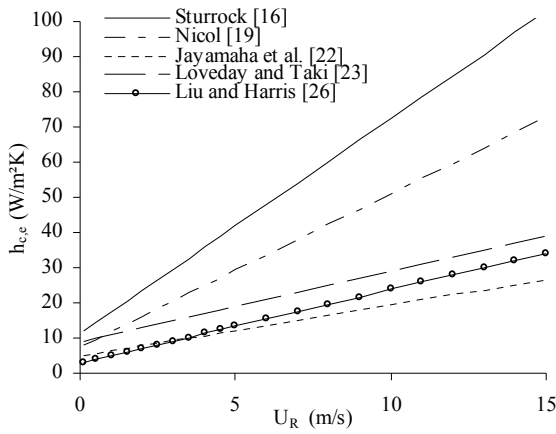

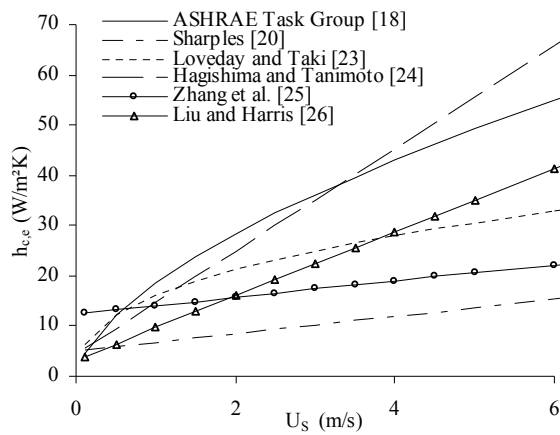Fig. 2. CHTC-U_R correlations for building facades from previous research.

Fig. 3. CHTC-U_S correlations for building facades from previous research.

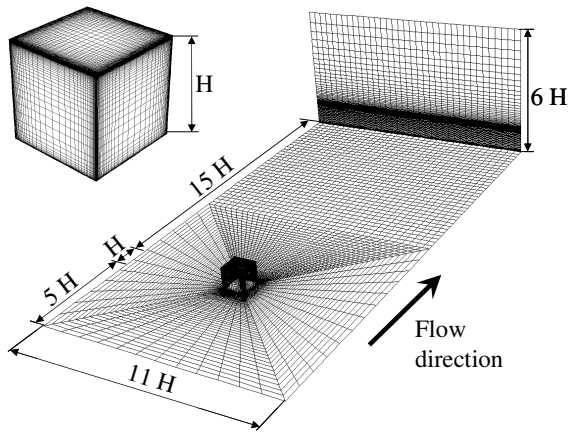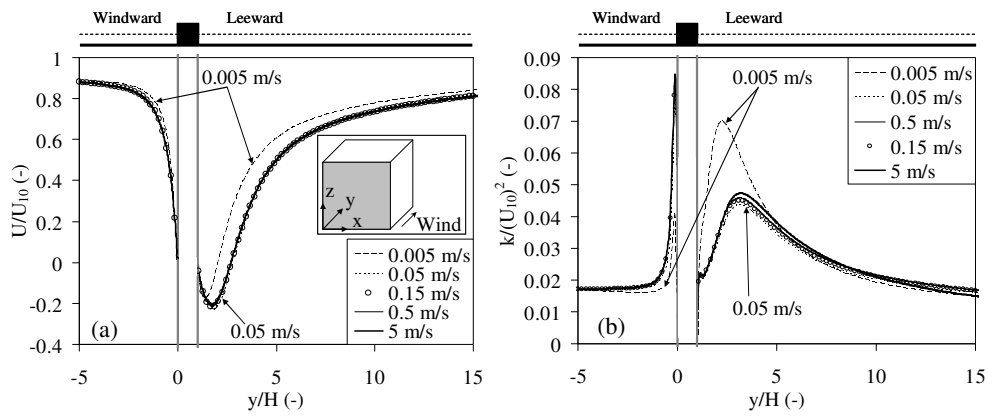Fig. 4. Computational domain and grid (H = 10 m).

Fig. 5. Profiles of dimensionless horizontal wind speed (a) and turbulent kinetic energy (b) along a centreline ((x,z) = (5,5)) through the building (grey area = windward surface) for different wind speeds (U_{10}).
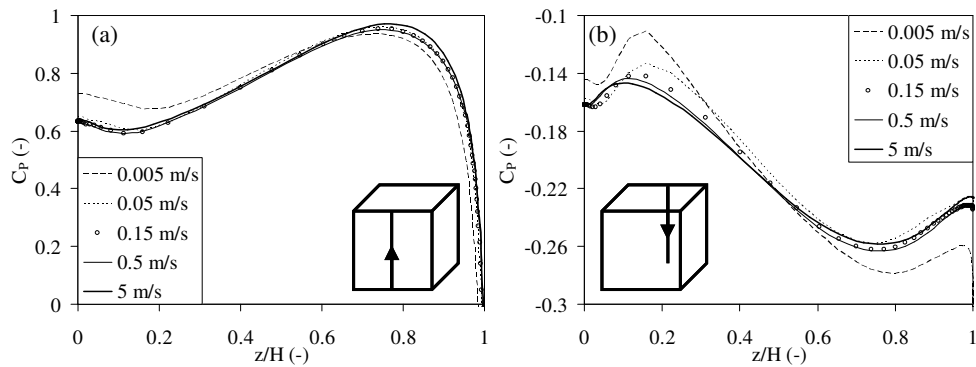

Fig. 6. Pressure coefficient distribution in a vertical centreplane on the windward (a) and leeward (b) surfaces for different wind speeds (U_{10}).
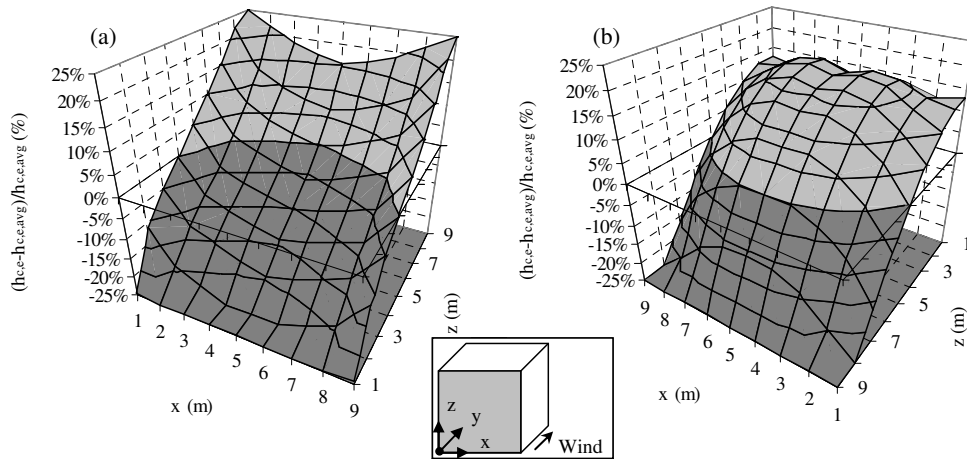
Fig. 7. Dimensionless CHTC distribution over windward (a) and leeward (b) surfaces.

Fig. 8. CHTC-U_{10} correlation: Distribution of coefficient A and exponent B (Eq.(6)) over windward surface (coordinate system same as in Fig.7). Note that the z-axis in Figure 8(b) is reversed compared to that in Figure 8(a).
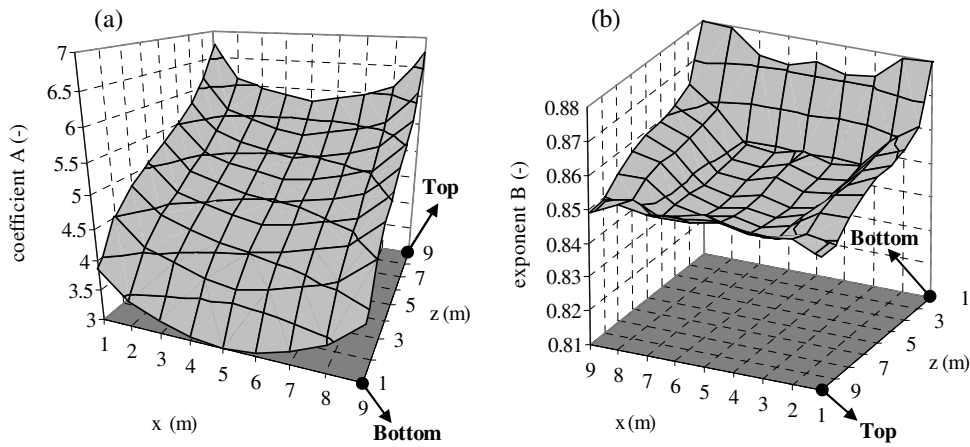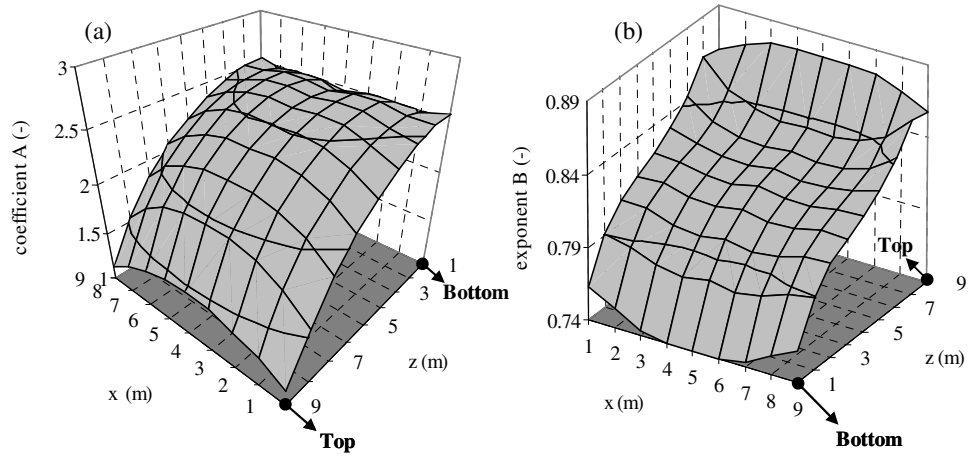
Fig. 9. CHTC-U_{10} correlation: Distribution of coefficient A and exponent B (Eq.(6)) over leeward surface (coordinate system same as in Fig.7). Note that the z-axis in Figure 9(b) is reversed compared to that in Figure 9(a).

Table 1. CHTC-U correlations derived from full-scale measurements on building facades.

Author	Building geometry	Value	Location	Range (m/s)	Surface	Correlations of CHTC
	Length x Width x Height (m)					
Gerhart [15]	Building, 30 m high	U_R	6 m above roof	-	-	([c])
Sturrock [16]	Tower, 26 m high	U_R	-	-	WW	$6.1\ U_R+11.4$
Ito et al. [17]	Open L-shaped building, 18 m high	U_S	0.3 m from facade	0.5-3.5	WW+LW	-
		U_R	8 m above roof	0.5-13	WW+LW	-
ASHRAE Task Group [18] (derived from Ito et al. [17])	-	U_S	0.3 m from facade	-	WW+LW	$18.6U_S^{0.605}$
					WW	$U_S=0.25\ U_{10}$ ($U_{10} > 2$ m/s) $U_S=0.5$ ($U_{10} < 2$ m/s)
					LW	$U_S=0.05\ U_{10}+0.3$
Nicol [19]	Rectangular building	U_R	-	0-5	WW+LW	$4.35\ U_R+7.55$
Sharples [20] ([b])	Tower (20x36x78 m)	U_S	1 m from facade	0.5-20	WW+LW	$1.7\ U_S+5.1$ ([a])
		U_{10}		0-12	WW	$2.9\ U_{10}+5.3$ ([a])
					LW	$1.5\ U_{10}+4.1$ ([a])
Yazdanian and Klems [21]	Small, single storey, rectangular building	U_{10}		0-12	WW	$\sqrt{(0.84\Delta T^{1/3})^2+(2.38U_{10}^{0.89})^2}$
					LW	$\sqrt{(0.84\Delta T^{1/3})^2+(2.86U_{10}^{0.617})^2}$
Jayamaha et al. [22]	Vertical wall (1.2x1.8 m)	U_R	above vertical wall	0-4	WW+LW	$1.444\ U_R+4.955$
Loveday and Taki [23]	Rectangular building with L-shaped ground floor (21x9x28 m)	U_S	1 m from facade	0.5-9	WW LW	$16.15U_S^{0.397}$ $16.25U_S^{0.503}$
		U_R	11 m above roof	0.5-16	WW LW	$2.00\ U_R+8.91$ $1.77\ U_R+4.93$
Hagishima and Tanimoto [24]	Two adjacent rectangular buildings (16.6x26.8x16.5 m + 22.2x15.3x9.9 m)	U_S	0.13 m from facade/roof	0.5-3	RF	$3.96\sqrt{\overline{u}^2+\overline{v}^2+\overline{w}^2+2k}+6.42$
					WW+LW	$10.21\sqrt{\overline{u}^2+\overline{v}^2+\overline{w}^2+2k}+4.47$
Zhang et al. [25]	Small building (3x3x3 m)	U_S	0.2 m from facade	1-7	WW+LW	$-0.0203\ U_S^2 + 1.766\ U_S + 12.263$
Liu and Harris [26] ([b])	Rectangular building (8.5x8.5x5.6 m)	U_S	0.5 m from facade	0-3.5	WW LW	$6.31\ U_S+3.32$ $5.03\ U_S+3.19$
		U_R	1 m above roof	0-9	WW LW	$2.08\ U_R+2.97$ $1.57\ U_R+2.66$
		U_{10}		0-16	WW LW	$1.53\ U_{10}+1.43$ $0.90\ U_{10}+3.28$

WW: Windward (incidence angles (angle between approach flow wind direction and the normal to the windward surface) from -90° to 90°), LW: Leeward (remainder of incidence angles), RF: Roof, ΔT: Temperature difference between exterior surface and environment, $\overline{u}, \overline{v}, \overline{w}$: x, y, z components of mean wind speed, k: turbulent kinetic energy, ([a]): edge site on 18th floor of the tower, ([b]): More correlations are provided in the original paper but are not given here for the sake of brevity, ([c]): No consistent correlation could be obtained.

Table 2. CHTC-U correlations derived from wind-tunnel experiments on bluff bodies placed in a turbulent boundary layer.

Author	Measuring technique	Approach flow	Incidence angle	Reference velocity	Reynolds number range ([a])	Correlations of surface-averaged CHTC			
						Front	Rear	Side	Top
Sturrock [16]	-	Laminar flow	0°-90°	FS	4.7x10^4 - 15.7x10^4	$h_{c,e}=5.7U_\infty+23$	-	-	-
Chyu and Natarajan [35]	NS ([b])	Turbulent, BL thickness ±¼ of cube height	0°	FS	3.1x10^4 - 11x10^4	$Sh=0.868Re^{0.538}$	$Sh=0.196Re^{0.661}$	$Sh=0.278Re^{0.652}$	$Sh=0.247Re^{0.657}$
Natarajan and Chyu [36] ([c])	NS ([b])	Turbulent, BL thickness ±¼ of cube height	0°-10°-25°-45°	FS	3.1x10^4 - 11x10^4	Front surface (for 45°): $Sh= 1.77Re^{0.637} Sc^{1/3}$ (Correlations for other surfaces and wind directions: see original paper)			
Quintela and Viegas [37] ([c])	FM	Turbulent, BL thickness 0.33-0.6 of cube height	0°-45°	FS	5.2x10^3 - 37x10^3	Cube-averaged value (for 0°): $Nu = 0.32Gr^{0.27}(1+1.15\frac{Re}{\sqrt{Gr}})$			
Meinders et al. [39]	IT	Developing turbulent channel flow	0°	Bulk velocity	2.75x10^3 - 4.97x10^3	Cube-averaged value $Nu=ARe^{0.65}$			
Nakamura et al. [40]	TC	Turbulent, BL thickness 1.5-1.83 of cube height	0°	FS	4.2x10^3 - 33x10^3	$Nu=0.71Re^{0.52}$	$Nu=0.11Re^{0.67}$	$Nu=0.12Re^{0.70}$	$Nu=0.071Re^{0.74}$
Nakamura et al. [41]	TC	Turbulent, BL thickness 1.5-1.83 of cube height	45°	FS	4.2x10^3 - 33x10^3	$Nu=0.52Re^{0.55}$	$Nu=0.11Re^{0.67}$		$Nu=0.029Re^{0.84}$
Wang and Chiou [42]	NS ([b])	Fully-developed channel flow	0°	MVI	8.0x10^2 - 5.0x10^3	$Sh=0.961Re^{0.529}$	$Sh=0.223Re^{0.637}$	$Sh=0.102Re^{0.663}$	$Sh=0.305Re^{0.639}$

NS: Naphthalene Sublimation, IT: Infrared Thermography, TC: ThermoCouples, FM: Flux Meters, FS: Free-Stream velocity, MVI: Maximum Velocity at Inlet, BL: Boundary Layer, Gr: Grashof number, A: parameter, ([a]): based on cube height and reference velocity (e.g. FS), ([b]): The CHTC can be derived from the heat and mass transfer analogy (Sh: Sherwood number, Sc: Schmidt number = 1.87 for the experimental conditions), ([c]): More correlations are provided in the original paper but are not given here for the sake of brevity.

Table 3. Surface-averaged CHTC-U_{10} correlations from CFD simulations ([a]: More correlations are provided in the original paper but are not given here for the sake of brevity).

Author	Building geometry Length x Width x Height (m)	U_{10} range (m/s)	Correlation of surface-averaged CHTC for windward surface (W/m²K)
Emmel et al. [46] [a]	Rectangular building (6x8x2.7 m)	1 - 15	$h_{c,e}=5.15U_{10}^{0.81}$ (short wall) $h_{c,e}=4.84U_{10}^{0.82}$ (long wall)
Blocken et al. [47] [a]	Cubic building, 10 m high	1 - 4	$h_{c,e}=4.6U_{10}^{0.89}$
Defraeye et al. [48]	Cubic building, 10 m high	0.05 - 5	$h_{c,e}=5.15U_{10}^{0.82}$

Table 4. Critical Reynolds numbers.

Author	Critical Reynolds number
Hoydysh et al. [68]	3400
Castro and Robins [69]	4000
Cherry et al. [70]	30000
Ohba [71]	2100
Djilali and Gartshore [72]	25000
Snyder [73]	4000
Mochida et al. [74]	7500
Uehera et al. [75]	3500-8000

Table 5. Percentage difference ($|h_{c,e,avg,corr}-h_{c,e,avg}|/h_{c,e,avg}$) of different CHTC-$U_{10}$ correlations with CHTC data ($h_{c,e,avg}$ is the surface-averaged CHTC from the numerical simulation, $h_{c,e,avg,corr}$ is the surface-averaged CHTC using a specific CHTC-U_{10} correlation of one of the different cases). Small differences (≤ 5 %) are highlighted.

Wind speed (m/s)	Correlations using different sets of velocities (U_{10})					
	Case A (0.15-0.5-1-2.5-5-7.5 m/s)	Case B (0.05-0.15-0.5 m/s)	Case C (0.15-0.5 m/s)	Case D (0.15-0.5-1 m/s)	Case E (0.5-1 m/s)	Case F (0.5-2.5 m/s)
0.05	16 %	2 %	8 %	10 %	17 %	19 %
0.15	3 %	3 %	0 %	0 %	5 %	6 %
0.5	2 %	1 %	0 %	1 %	0 %	0 %
1	3 %	7 %	3 %	1 %	0 %	1 %
2.5	1 %	15 %	8 %	5 %	2 %	0 %
5	1 %	21 %	13 %	9 %	4 %	1 %
7.5	2 %	25 %	15 %	11 %	5 %	2 %
Correlation	$h_{c,e}=5.01U_{10}^{0.85}$	$h_{c,e}=4.56U_{10}^{0.77}$	$h_{c,e}=4.75U_{10}^{0.81}$	$h_{c,e}=4.85U_{10}^{0.82}$	$h_{c,e}=4.89U_{10}^{0.85}$	$h_{c,e}=4.93U_{10}^{0.86}$